

Pricing Using a Homogeneously Saturated Equation

Daniel T. Cassidy

Department of Engineering Physics,
McMaster University,
Hamilton, ON, Canada L8S 4L7

cassidy@mcmaster.ca

11 September 2011; revised 21 January 2013

Abstract

A homogeneously saturated equation for the time development of the price of a financial asset is presented and investigated for the pricing of European call options using noise that is distributed as a Student's t -distribution. In the limit that the saturation parameter of the equation equals zero, the standard model of geometric motion for the price of an asset is obtained. The homogeneously saturated equation for the price of an asset is similar to a simple equation for the output of a homogeneously broadened laser. The homogeneously saturated equation tends to limit the range of returns and thus seems to be realistic.

Fits to linear returns obtained from the adjusted closing values for the S&P 500 index were used to obtain best-fit parameters for Student's t -distributions and for normal distributions, and these fits were used to price options, and to compare approaches to modelling prices.

This work has value in understanding the pricing of assets and of European call options.

keywords: homogeneously saturated; pricing; European call options; Student's t -distribution; linear returns

1 Introduction

A homogeneously saturated equation for the time development of the price of a financial asset is presented and investigated for the pricing of European call options using noise that follows Student's t -distributions. Parameters for the Student's t -distributions were obtained by fitting to the linear returns calculated from the adjusted closing values of the S&P 500 Index over the period of 3 January 1950 to 27 July 2011. The homogeneously saturated equation for the price of an asset is similar to a simple equation for the output of a homogeneously broadened laser [1]. In the limit that the saturation parameter β of the homogeneously saturated equation equals zero, the standard solution of geometrical motion for the price of an asset is recovered.

The homogeneously saturated equation was obtained by constructing simple, coupled rate equations for the time development of the price of an asset and the supply of money. These equations were solved in a steady state approximation to obtain an equation for the time development of the price of an asset. The phenomenological approach is outlined in the Appendix and is presented in [2]. Analytic solutions to a homogeneously saturated model, which is coupled, non-linear differential equations, were originally presented in 1984 [1].

In the text that follows, $S(t)$ is the value of an asset at time t , $S_0 = S(0)$ is the value of the asset at $t = 0$, α is a drift rate, σ is a scale parameter, $f(t)$ is a noise driving term and is a stochastic process, and β is a saturation parameter.

In a Langevin approach, the equation for the time development of the value of an asset from a homogeneously saturated model is

$$\frac{d}{dt}S(t) = \frac{\alpha S(t) + \sigma S(t) f(t)}{1 + \beta S(t)}. \quad (1)$$

In the development of the Eq. (1), a reservoir for money was assumed and the noise was ascribed to fluctuations in the amount of money available to invest in the asset. This is

24 consistent with market microstructure studies [3–6]. In these studies, it was revealed that
 25 the order book for the market is sparse, that price jumps occur when the orders are filled
 26 across gaps in the order book, that the stability of markets relies on a delicate balance
 27 between supply and demand, and that the need to store supply and demand to enable
 28 trading leads to structure in the pricing. These studies show elements of a reservoir, of a
 29 coupling between price and supply, and of fluctuations in the money available in the order
 30 book causing fluctuations in the price, similar to the phenomenological elements that lead
 31 to a homogeneously broadened equation for the price of an asset.

32 The value of the asset at time t , $S(t)$, is found through solution of the Langevin equation
 33 for the homogeneously saturated model, Eq. (1), to be

$$S(t) = \frac{S_o e^{\int_0^t \alpha + \sigma f(\eta) d\eta}}{e^{\beta(S(t) - S_o)}} = \frac{S_o e^{\alpha t + W(t)}}{e^{\beta(S(t) - S_o)}} , \quad (2)$$

34 a transcendental equation that can be solved for $S(t)$ given α , β , S_o , and $W(t) = \int_0^t \sigma f(\eta) d\eta$.
 35 The simple dependence on the stochastic process $W(t)$ makes simulation straight forward.

36 By comparison, in a Langevin approach the standard model for the time development of
 37 the value of an asset is

$$\frac{d}{dt}S(t) = \alpha S(t) + \sigma S(t) f(t) \quad (3)$$

38 with solution

$$S(t) = S_o \exp \int_0^t (\alpha + \sigma f(\eta)) d\eta = S_o \exp(\alpha t + W(t)) . \quad (4)$$

39 If the noise driving term $f(t)$ is a normally distributed process, then the solution to the
 40 standard model is geometrical Brownian motion.

41 The standard model is obtained from the homogeneously saturated equation in the limit
 42 that the saturation parameter β equals zero.

43 Numerous revert-to-mean models for the time development of the price of an asset, of
44 volatility, and of interest rates have been put forth and analyzed. Anteneodo and Riera [7]
45 and Wu et al. [8] have listed some of these models and have shown that these models can be
46 incorporated in a single stochastic differential equation by choice of parameters in the single
47 differential equation.

48 It is doubtful that a simple revert-to-mean feature is of much benefit when the noise
49 driving term is drawn from a fat tailed distribution. The standard model implicitly has a
50 revert-to-mean feature; a revert-to-mean value of zero, which is the mean value of the noise
51 distribution and which is implicit in each model. If the noise drives the output to a large
52 value with a revert-to-mean of zero, then the noise will also drive the output to a large value
53 when the revert-to-mean value is finite and non-zero. Anteneodo and Riera [7] have shown
54 that nonlinear additive-multiplicative processes are necessary to provide realistic descriptions
55 of observations.

56 Smith et al. [4] used a rate equation for the density of the order book and non-linear
57 feedback to investigate how prices depend on the rate of flow of orders. The authors were
58 able to explain the concavity of the price impact function, the existence of universal supply
59 and demand functions, and the average daily spread. Their model did not include coupled
60 rate equations.

61 The homogeneously saturated equation presented in this paper is based on phenomeno-
62 logical, coupled rate equations for the time development of a reservoir of money and of the
63 price of an asset. The rate equation for the reservoir of money has a revert-to-pumping-rate
64 feature, where the pumping rate is the rate at which money flows into the reservoir to sup-
65 port the price. The rate equation for the reservoir of money also has a stochastic driving
66 term to account for fluctuations. The steady state solution to the coupled equations has
67 some interesting and realistic features. The equation tends to produce a linear relationship
68 between the input and output, and to limit the range of the output for a given input. Both

69 of these tendencies mean that the price of an asset is less likely than the standard model to
70 wander off to infinity and that integrals required to price options can be evaluated for many
71 fat-tailed distributions.

72 The price of an European call option at time T can be found from the arbitrage theo-
73 rem [9–11] as $E\{\max(S_T - K_T, 0)\}$ where $S_T = S(T)$ is the fair price of the asset at time T ,
74 K_T is the strike price at time T , and $E\{\max(x, y)\}$ is the expectation of the maximum value
75 of the set $\{x, y\}$ [12]. The constraint of a fair price for S_T requires that $S(t)$ be a martin-
76 gale. It is not necessary to solve a differential equation to find the price of an European call
77 option [12–14]. The arbitrage theorem approach gives the same answer as the Black-Scholes
78 equation in the limit that the returns are normally distributed [12].

79 In this paper the time development of the price of an asset and the pricing of European
80 options based on a homogeneously saturated equation are considered. Section 2 provides
81 information on solutions to the homogeneously saturated equation and on simulations. Sec-
82 tion 3 provides fits to returns for the S&P 500 data. Section 4 provides information on
83 pricing using the fits from Sec. 3. Section 5 is a conclusion and Sec. 6 is an Appendix that
84 outlines a derivation of the homogeneously saturated equation. The starting point for this
85 paper is the solution to the homogeneously saturated equation. The Appendix is not a rig-
86 orous derivation of the underlying equations. The Appendix is meant as a phenomenological
87 justification for the starting point for this paper, which is the solution to a homogeneously
88 saturated equation for the time development of the price of an asset.

89 In this paper, time is represented by t and the ‘ t ’ in the Student’s \mathbf{t} –distribution is set
90 in bold.

91 2 Homogeneously Saturated Equation

92 Figure 1 is comprised of plots of the solution $S(x)$ to the homogeneously saturated equation,
 93 Eq. (2), as a function of the input $x = \alpha t + W(t)$ for selected values of the saturation param-
 94 eter β . The shapes of the solutions for various values of β are important in understanding
 95 the properties of the solution. For small values of the saturation parameter β the solution
 96 $S(x)$ appears to be exponential with x whereas for large values of the saturation parameter
 97 the solution is essentially linear in x , with decreasing slope as β increases. The exponential
 98 increase with x for small β is consistent with the solution to the standard model, Eq. (4).

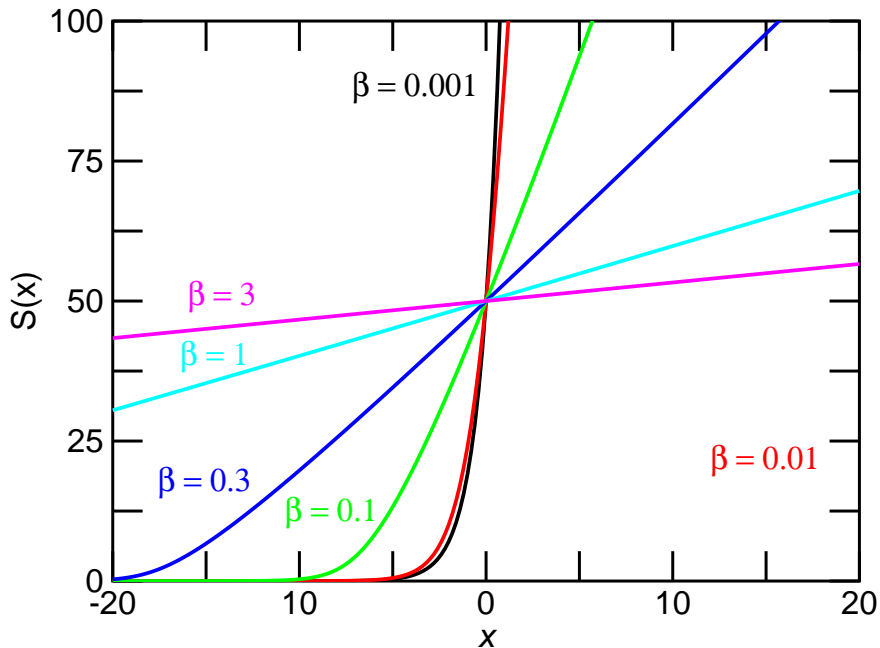


Figure 1: Solutions $S(x)$ to the homogeneously saturated equation as a function of the input $x = \alpha t + W(t)$

99 Table 1 gives descriptive statistics for solutions $S(x)$ to Eq. (2) for various values of
 100 the saturation parameter β to the homogeneously saturated equation for 131072 random
 101 draws from a Student's t -distribution with shape parameter $\nu = 3$ and for 131072 random
 102 draws from a normal distribution. The draws from the normal and the $\nu = 3$ Student's

103 t -distributions are the values for the sum of the drift and noise driving term, $x = \alpha t + W(t)$,
 104 in the equation for the price $S(x)$, Eq. (2). The same set of random numbers were used
 105 for each value of β but different sets were used for the normal and t -distributions. The
 106 scale parameters were adjusted, by multiplying the input noise by an appropriate factor, for
 107 each β to give the same standard deviation for $S(t)$. This was done to enable comparison.
 108 The standard deviation of the daily returns is observable. The noise required to achieve the
 109 observed standard deviation is not known *a priori* in the homogeneously saturated equation.

110 For the simulations reported in Table 1, $S_T = S_o \exp(rT)$ was set equal to $50.00 \exp(+0.03)$
 111 $= 51.523$ and the standard deviation of the solution to Eq. 2, $S(t)$, was set to $S_T \times 0.3 \times$
 112 $\sqrt{\nu/(\nu - 2)}$, or 26.78 for $S(t)$ found with the Student's t -distribution driving noise and
 113 15.46 for $S(t)$ found from the normally distributed noise. For a normal distribution, $\nu = \infty$,
 114 and $\sqrt{\nu/(\nu - 2)} = 1$. The numbers were chosen to demonstrate pricing with $T = 1$ year, the
 115 risk free rate $r = 0.03$, the annualized volatility $= 0.3$, and a very fat-tailed noise distribution
 116 with $\nu = 3$ degrees of freedom (or a shape parameter $\nu = 3$). The Black Scholes formula sets,
 117 under these conditions, a price of $C_o = \$7.12$ for an European call option with $K_T = \$49.00$.
 118 Also given in the Table 1 are values from the Monte Carlo simulations for the prices of an
 119 European call option for the various values of β . The Black-Scholes price is given as point of
 120 reference only. There are differences in approaches that lead to the Black-Scholes equation
 121 and to the homogeneously saturated equation, and these differences make direct comparisons
 122 difficult. See later in this Section for a discussion of noise rectification, of returns, and of
 123 volatility and standard deviation.

124 The 131072 samples for the input noise from the $\nu = 3$ Student's t -distribution had
 125 a mean of 7.72×10^{-4} , a standard deviation of $1.701 \approx \sqrt{\nu/(\nu - 2)} = \sqrt{3}$, a minimum
 126 value of -46.4 , a maximum value of 53.9 , a skewness of 0.085 , and a kurtosis of 39.9 . The
 127 131072 samples for the input noise from the normal distribution had a mean of -3.0×10^{-3} , a
 128 standard deviation of 1.000 , a minimum value of -4.67 , a maximum value of 4.39 , a skewness

Table 1: Descriptive statistics for $S(t)$ from a homogeneously saturated equation with Student's t and normally distributed noises. The costs C_o of European call options with $S_o = 50.0$, $K_T = 49.0$, $T = 1$ year, $r = 0.03$, and volatility = 0.3 are also given for the two noise sources.

	$\beta = 0.001$	$\beta = 0.01$	$\beta = 0.1$	$\beta = 0.3$	$\beta = 1.0$	$\beta = 3.0$
t with $\nu = 3$						
min	0.02	0.0	0.0	0.0	0.0	0.0
average	53.6	54.7	53.3	52.8	52.6	52.5
max	4809	1902	1138	1055	1023	1013
kurtosis	9211	334	55	42	38	37
skewness	67	9.3	3.1	2.6	2.4	2.3
input scale	0.172	0.410	2.07	5.64	18.1	53.6
C_o	\$5.91	\$8.62	\$10.04	\$10.21	\$10.27	\$10.29
normal						
min	13	9.6	1.28	0.0	0.0	0.0
average	53.5	53.0	51.9	51.6	51.5	51.5
max	170	146	125	121	120	120
kurtosis	4.2	3.4	2.9	2.9	3.0	3.0
skewness	0.83	0.56	0.16	0.07	0.02	0.005
input scale	0.300	0.451	1.87	4.97	15.8	46.7
C_o	\$7.03	\$7.16	\$7.28	\$7.29	\$7.29	\$7.29

129 of -0.008 , and a kurtosis of 3.01 . For a Student's t -distribution, which has support over
 130 $[-\infty, +\infty]$, the coefficient of skewness equals zero and exists for $\nu > 3$, and the coefficient of
 131 kurtosis equals $3(\nu - 2)/(\nu - 4)$ and exists for $\nu > 4$. The skewness and kurtosis exist for all
 132 values of the shape parameter ν if the fat tails of the Student's t -distribution are removed
 133 by truncation [15].

134 Note that there is minimal noise rectification (i.e., the mean value for $S(t)$ does not have
 135 an $\exp(+\sigma^2/2)$ enhancement) for a heavily saturated system, and that the homogeneously
 136 saturated model shows a reduction of the maximum value for $S(t)$ as β increases. As β
 137 increases, C_o , the price of a European option, approaches the Black Scholes value of $\$7.12$
 138 for simulations that draw from a normal pdf. In the calculation of C_o , the mean and the
 139 standard deviation were forced through an iterative procedure to equal $S_o \exp(0.03)$ and
 140 $S_T \times 0.3 \times \sqrt{\nu/(\nu - 2)}$. The stopping criterion for the iterative procedure was that the
 141 absolute value of the difference between the standard deviation for the solution to $S(t)$ and
 142 the target standard deviation was < 0.0005 . Pricing with realistic inputs, rather than with
 143 input parameters chosen to demonstrate the differences, is given in Sec. 4.

144 The rows of Table 1 that are labelled "input scale" give the scale factors that were
 145 required to achieve the target standard deviation of $S(t)$. The reason for the different input
 146 scales to obtain the target standard deviation for the output $S(x)$ can be observed from Fig.
 147 1. For small β and for $x = \alpha t + W(t) > 0$, $S(x)$ is a very steep function of x , and only
 148 small amplitudes for the input noise x are required to give a large standard deviation for the
 149 output $S(t)$. For large β and x such that $S(x) \gg 0$, $S(x)$ is, to a good approximation, a linear
 150 function of x with a small slope, and large amplitudes for the input noise x are required to
 151 achieve a large standard deviation for the output $S(x)$. For x such that $S(x) \gg 0$, the slope
 152 of $S(x)$ approaches $1/\beta$. This means that the output is compressed for a heavily saturated
 153 system (i.e., for a system characterized by a large β). Large changes in x produce small
 154 changes in $S(x)$ for large β and for $S(x) \gg 0$.

155 Figure 1 can also be used to explain the noise rectification properties. For the normal
 156 data, the input noise (before the input scale is applied) is confined in the range $-4.67 \leq$
 157 $x \leq 4.39$. The noise seldom pushes the solution $S(x)$ into the highly nonlinear region where
 158 $S(x) \approx 0$. As a result, the pdf for $S(x)$ is approximately symmetric and centred around
 159 $x = 0$; see the summary statistics for the normally distributed input of Table 1. For the
 160 fat-tailed distribution, the input noise (before the input scaling is applied) is in the range
 161 $-46.4 \leq x \leq 53.9$, and the noise often pushes the solution $S(x)$ into the nonlinear region
 162 where $S(x) \approx 0$ and this distorts the pdf for $S(x)$, which leads to an increase of the mean
 163 value of the output. For increasing β , $S(x)$ is an approximately linear function of x over a
 164 greater range of x , and the contribution to the mean from the noise rectification drops. For
 165 small values of the input noise (the shape and scale parameters of Table 1 were chosen to
 166 highlight the effects), the noise rectification will be small or negligible, particularly as the
 167 transfer function for $S(x)$ becomes linear with increasing saturation parameter β .

168 Figures 2 and 3 are histograms of $S(x)$ for $\beta = 0.3$ and 0.01 for 8192 draws from the
 169 same $\nu = 3$ Student's t -distribution with a scale parameter equal to 0.3 . The solid curves
 170 are $\nu = 3$ Student's t -distributions with the standard deviations matched to the standard
 171 deviations of the solutions $S(x)$ for $\beta = 0.3$ and 0.01 . The histograms show the asymmetry
 172 in the solution for small saturation parameter β and the symmetry in the solution for large β
 173 and small noise. The mean of $S(x) - S_o$ for $\beta = 0.01$ was 14.4 whereas the mean of $S(x) - S_o$
 174 for $\beta = 0.3$ was -0.0024 . For $\beta = 0$, which is a log Student's t -distribution, the mean value
 175 was 3.7×10^5 with a minimum value of 0.0 and a maximum value of 1.7×10^9 for the same
 176 noise driving terms for the 8192 simulations. The homogeneously saturated equation limits
 177 the range of values and the noise rectification compared to the standard model (for which
 178 $\beta = 0$).

179 In this work the n -day per mille return $R_n(t)$ has been defined as $1000 \times (S(t+n)/S(t) - 1)$

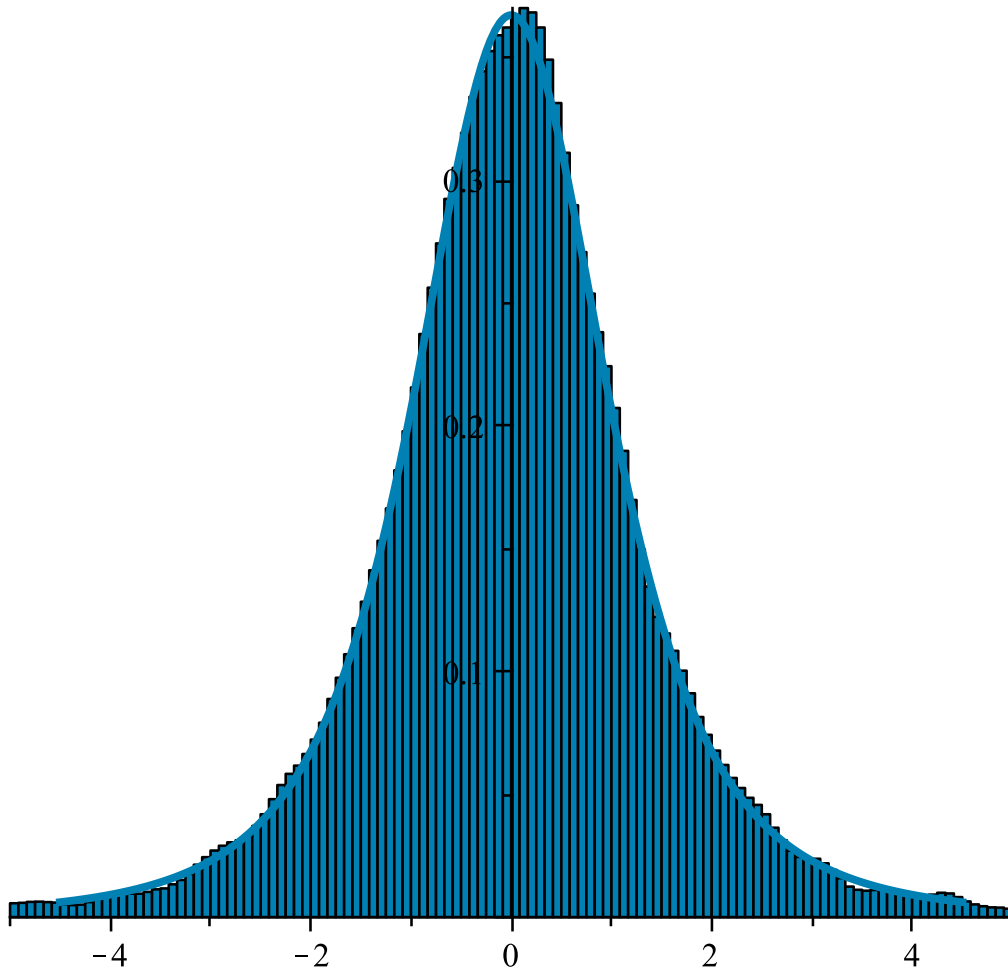


Figure 2: $\beta = 0.3$ histogram and Student's t -distribution

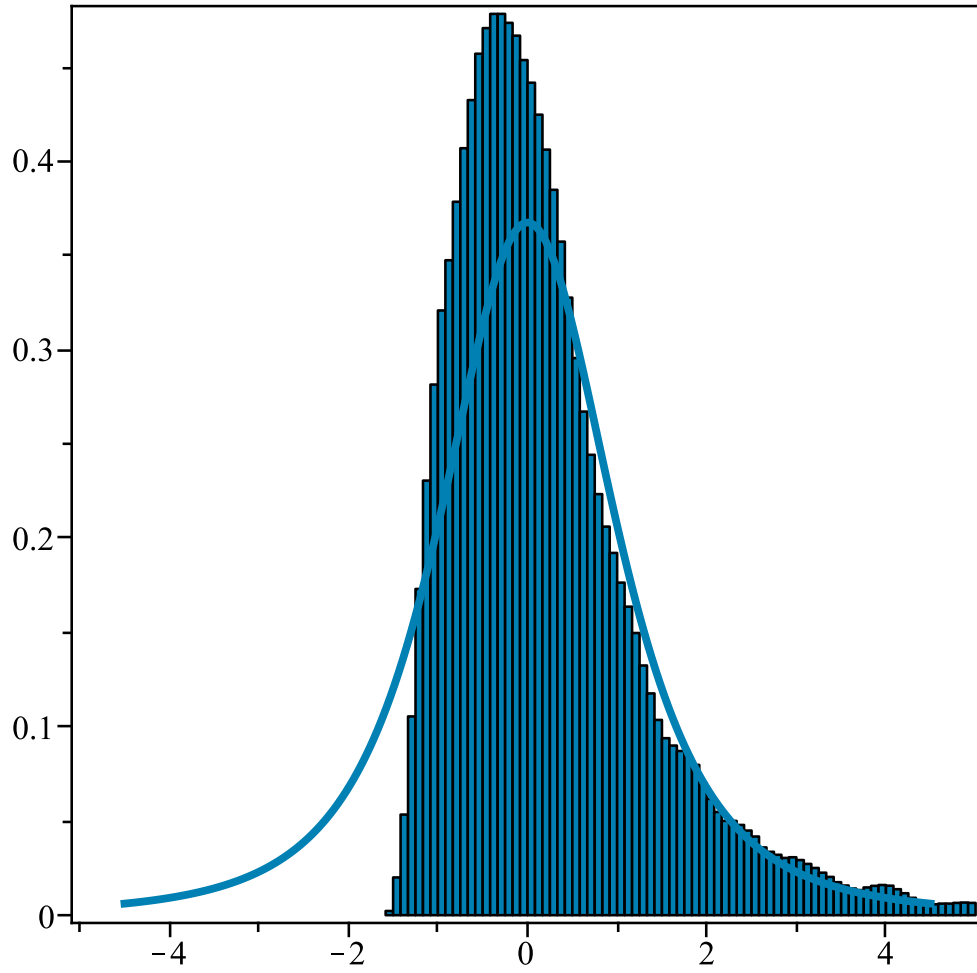


Figure 3: $\beta = 0.01$ histogram and Student's t -distribution

180 where time t and n are measured in days. The multiplicative factor of 1000 transforms the
 181 return into a per mille return. The definition of the n -day return is in contrast to the more
 182 common n -day return of $\ln(S(t+n)/S(t))$. Both definitions of the n -day return give the
 183 same answer for small deviations of $S(t+n)$ about $S(t)$, as can be observed in Fig. 4. For
 184 small changes, $\ln(S(t+n)/S(t)) = \ln(S(t)(1+\varepsilon)/S(t)) = \ln(1+\varepsilon) \approx \varepsilon - \varepsilon^2/2 + \varepsilon^3/3$ and to
 185 first order, the logarithmic return is linear in ε . There are several reasons for preferring the
 186 n -day linear return as defined here. Returns are known to be fat tailed; the changes about
 187 $S(t)$ might not always be small. The logarithmic form of the return permits returns that
 188 are $< -100\%$, as shown in Fig. 4. A return of $< -100\%$ makes little sense. The logarithmic
 189 return makes some sense in the standard model; $\ln(S(t)) = \alpha t + W(t)$ gives the sum of the
 190 noise $\sigma f(t)$ driving the process. If $S(t)$ is distributed as log-normal, then the logarithm of
 191 $S(t)$ is normally distributed. For a solution to a homogeneously saturated equation that
 192 is fully saturated, the transfer function is essentially linear – the output is to a very good
 193 approximation a linear function of the input, as shown in Fig. 1. A logarithmic return would
 194 then give in a homogeneously saturated approach a return that is the logarithm of the input
 195 noise, which would be acceptable (i.e., yield the same result as for the linear return $R_n(t)$)
 196 for small returns. However, the definition $R_n(t)$ works for all magnitudes of changes and
 197 does not give returns $< -100\%$, and thus seems preferable to the logarithmic definition.

198 In this work the volatility was taken as the scale parameter for the underlying distribution.
 199 For a normal distribution, the scale parameter is the standard deviation. For a Student's
 200 t -distribution, the standard deviation is a function of the shape parameter ν times the scale
 201 parameter, and is not equal to the scale parameter. A Student's t -distribution with shape
 202 parameter ν , scale parameter b , and location parameter (i.e., mean) equal to zero, can be
 203 written as

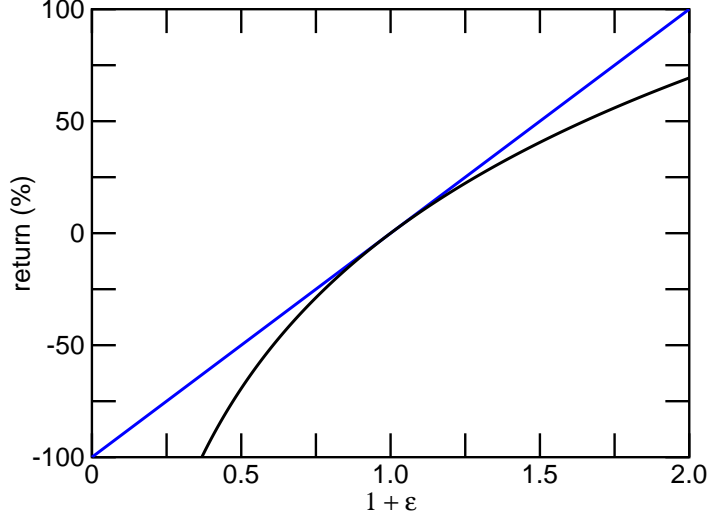


Figure 4: Linear return (straight line) and logarithmic return (curve) as a function of $S(t + 1)/S(t) = 1 + \varepsilon$. The minimum possible return is when $S(t + 1) = 0$, which occurs for $1 + \varepsilon = 0$.

$$f_{\mathbf{t}}(\xi, \nu, b) d\xi = \frac{\Gamma((\nu + 1)/2)}{\sqrt{\pi\nu}\Gamma(\nu/2)} \left(\frac{1}{1 + \xi^2/(\nu b^2)} \right)^{\frac{\nu+1}{2}} \frac{d\xi}{b} \quad (5)$$

204 where $f_{\mathbf{t}}(\xi, \nu, b) d\xi$ gives the probability of obtaining a value in the range ξ to $\xi + d\xi$ for a
 205 draw from a Student's \mathbf{t} -distribution with shape parameter ν , scale parameter b , and mean
 206 equal to zero.

207 For this \mathbf{t} -distribution the standard deviation equals $b \times \sqrt{(\nu/(\nu - 2))}$, and thus the
 208 standard deviation is the product of a scale factor (i.e., the volatility) and a function that
 209 accounts for the fat tails of the distribution. For large ν the Student's \mathbf{t} -distribution becomes
 210 a normal distribution, $\sqrt{(\nu/(\nu - 2))}$ is approximately equal to unity, and the volatility is
 211 approximately equal to the standard deviation. The dependence of the standard deviation on
 212 the volatility and a contribution from the shape of the underlying pdf might make estimation
 213 of the volatility from observations difficult. It might be necessary to eliminate the maximum
 214 and minimum values from a small size sample in an estimation of the volatility [16].

215 Figure 5 shows a comparison of a normal pdf with $\nu = 3$ Student's \mathbf{t} -distributions with

216 $b = 1$ and $b = 1/\sqrt{3}$. For these three functions, the standard deviations equal 1, $\sqrt{3}$, and 1.
 217 To compare prices based on Student's t -distributions and normal distributions, the correct
 218 volatility must be used.

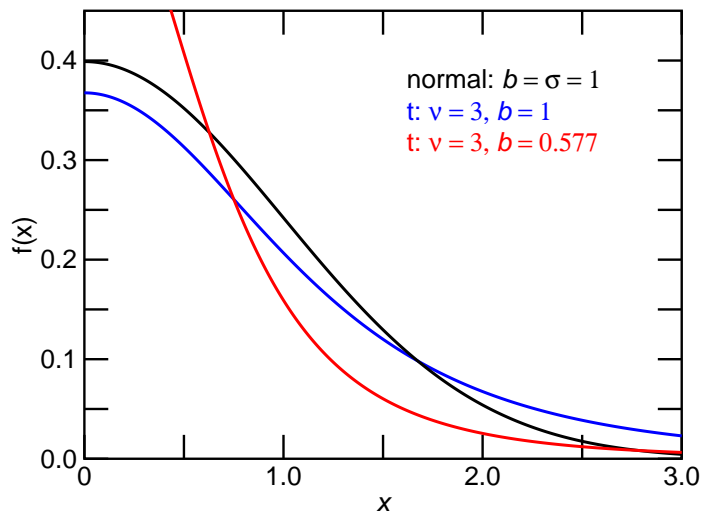


Figure 5: Comparison of a normal pdf, and $\nu = 3$ Student's t -distributions with $b = 1$ and with $b = 1/\sqrt{3}$.

219 3 Data

220 Figures 6, 7, 8 and 9 are semilog plots of the 1-day, 22-day, 44-day, and 88-day linear
 221 returns from the S&P 500 index from 3 January 1950 to 27 July 2011 with best fit Student's
 222 t -distributions and best fit normal distributions. The data are plotted as histograms without
 223 the vertical bars, hence the angular features in the plots of the data. Adaptable bin widths
 224 were used, with the requirement that at least 5 counts occur in each bin. The broad flat
 225 areas in the tails show the range of returns required to accumulate at least 5 counts. The
 226 thin lines plot, on linear scales, the cumulative density functions (CDF) for the data (in
 227 red), the t -distribution (in blue), and the normal distribution (in black). Only the CDFs
 228 from 0 to 0.1 and from 0.9 to 1.0 are shown. The CDF for the data and for a perfect fit

229 should overlap. The plots of the data, the fits, and the CDFs show that the data are fit well
 230 in the central region, with discrepancies in the tails. The quality of the fit of the Student's
 231 t -distribution to the 1-day returns is remarkable, as shown in Fig. 6.

232 It is interesting to note that the prices of European call options require the values of the
 233 asset and the probability of the asset for $S(T) > K_T$ where T is the expiration time of the
 234 asset and K_T is the value of the strike at time T . These values for the price of the asset and
 235 the probability are located on the right hand side of the plots, where the t -distribution fits
 236 well the data.

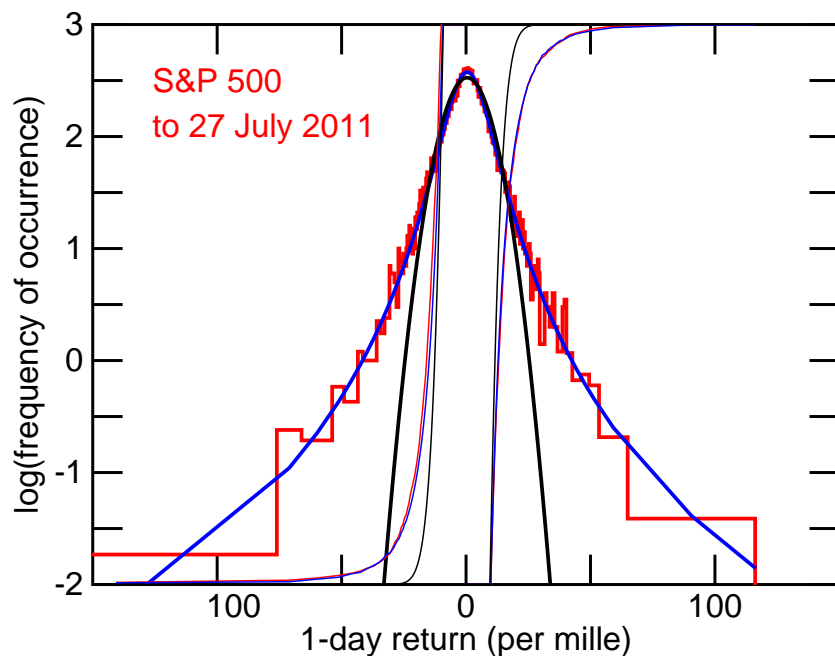


Figure 6: 1-day linear returns and fits of normal and Student's t -distributions to the 1-day linear returns.

237 Table 2 gives descriptive statistics and best fit parameters for per mille linear returns for
 238 the S&P 500 index from 3 January 1950 to 27 July 2011.

239 The uncertainties for the scale parameters are larger for fits to the Student's t -distributions
 240 than for the fits to the normal distributions. The fits to the t -distributions are not inferior

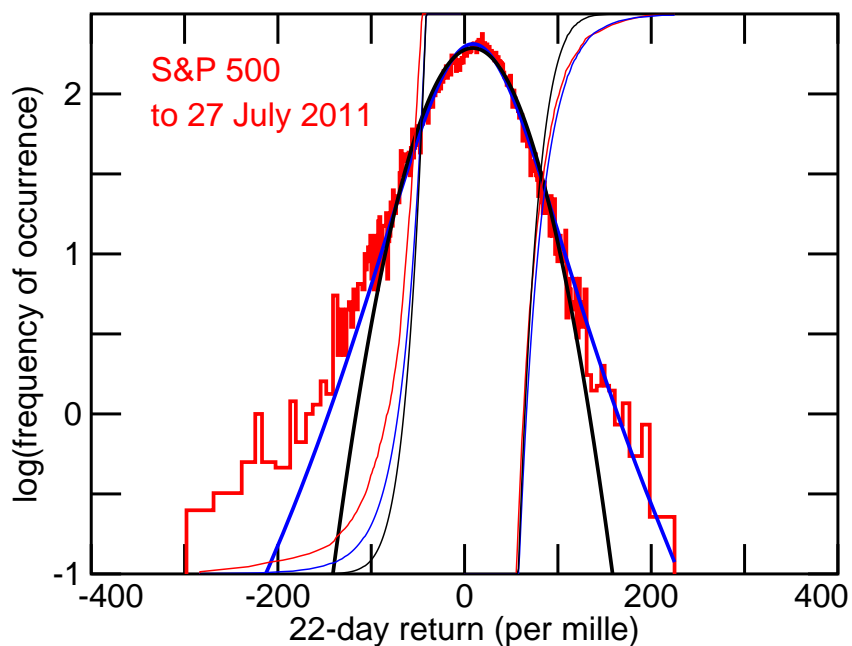


Figure 7: 22-day linear returns and fits of normal and Student's t -distributions to the 22-day linear returns.

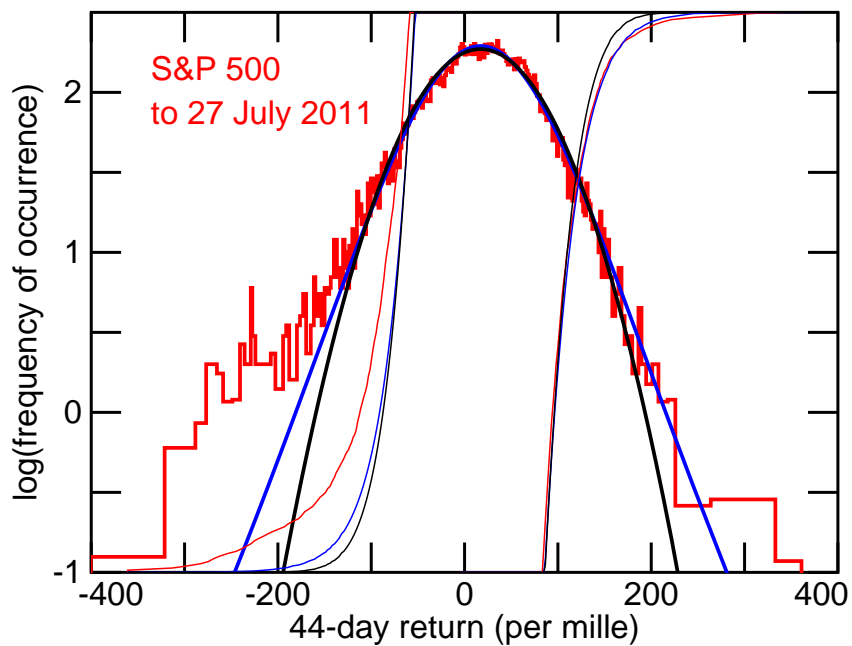


Figure 8: 44-day linear returns and fits of normal and Student's t -distributions to the 44-day linear returns.

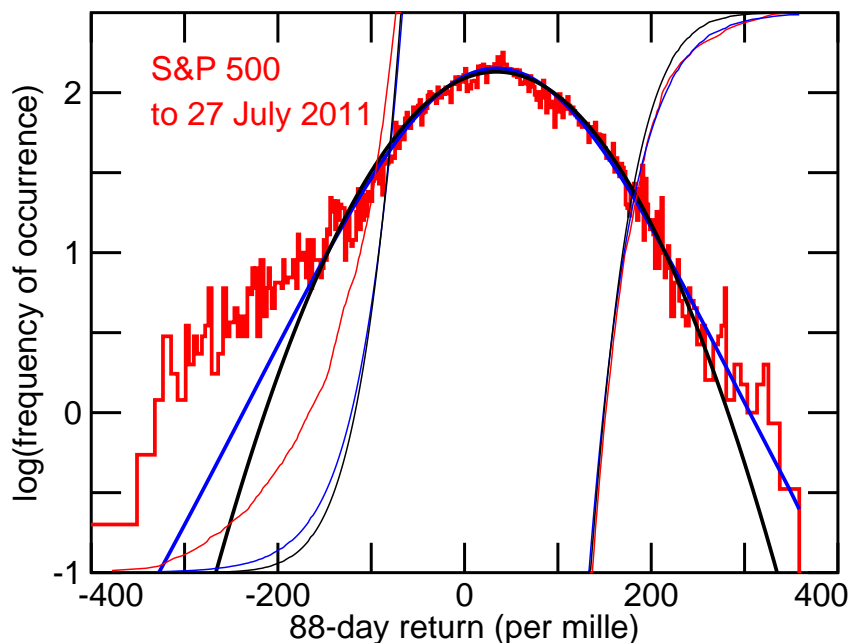


Figure 9: 88-day linear returns and fits of normal and Student's t -distributions to the 88-day linear returns.

Table 2: Descriptive statistics and best fit parameters for per mille linear returns, S&P 500 to 27 July 2011

	1-day	22-day	44-day	88-day	128-day
count	15491	15470	15448	15404	15364
min	-205	-298	-400	-403	-469
average	0.329	7.22	14.4	29.1	42.9
median	0.463	10.4	17.8	32.6	46.3
max	116	224	360	358	527
std dev	9.67	44.2	62.4	89.5	113
kurtosis	25	6.1	5.8	4.3	4.0
skewness	-0.7	-0.6	-0.6	-0.4	-0.3
t					
shape (ν)	3.33 ± 0.2	6.3 ± 0.7	9.0 ± 1.3	12.6 ± 3	12.0 ± 3
scale (b)	6.06 ± 0.3	34.7 ± 3	50.4 ± 4	73.9 ± 11	98 ± 11
location	0.46 ± 0.1	9.0 ± 0.6	16.9 ± 0.8	34.2 ± 1	45.8 ± 2
normal					
scale (σ)	7.3 ± 0.9	38.5 ± 0.4	54.5 ± 0.9	79.2 ± 0.7	104.6 ± 1
location	0.42 ± 0.2	8.8 ± 0.7	17.1 ± 0.5	34.2 ± 1	46.5 ± 2

241 to fits to the normal distributions. The shape and scale parameters are correlated in fits to
 242 the t -distributions. For a range of values it is possible to decrease one of the two correlated
 243 parameters, decrease the other, and still maintain a good fit.

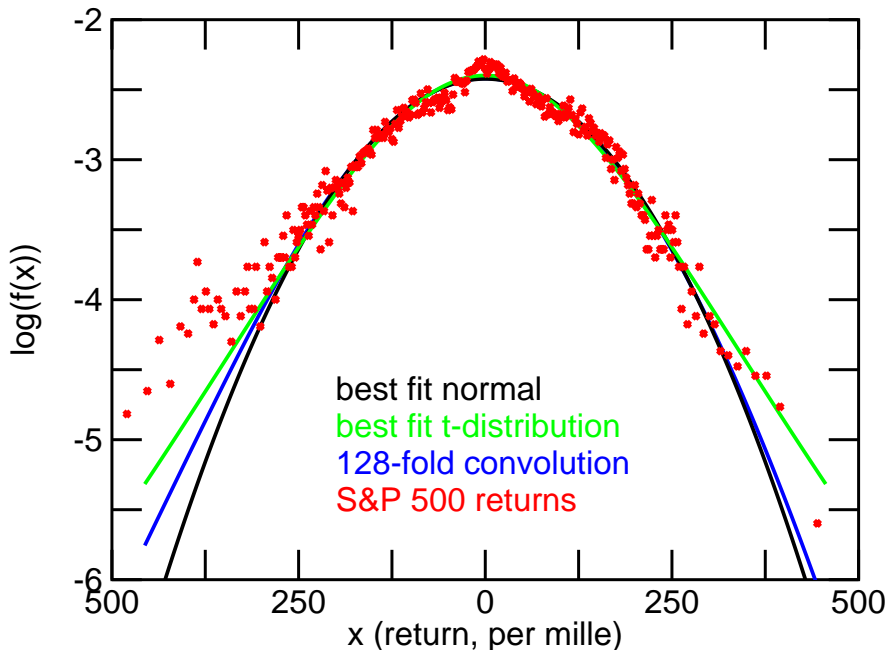


Figure 10: Best fits to the 128-day linear returns, data points, and 128-fold self-convolution.

244 Figure 10 is comprised of plots of the best fit normal pdf, best fit Student's t -distribution,
 245 the data points for the 128-day linear returns for the S&P 500 data minus the average
 246 return, and the 128-fold convolution of the best fit Student's t -distribution to the 1-day
 247 linear return for the S&P 500 data. The convolution was obtained by truncating the best
 248 fit t -distribution to the 1-day linear returns for $t < -305$ and $t > 116$. The minimum
 249 and maximum 1-day linear returns were -205 and 116 . The asymmetric truncation of the
 250 t -distribution leads to a slight asymmetry of the 128-fold convolution. This asymmetry
 251 can be observed by comparing the difference between the left and right tails of the best
 252 fit normal and the 128-fold convolution. The left truncation point of -305 was chosen
 253 to add some asymmetry, as the data show. Figure 10 shows that the 128-day return is

254 well approximated by the 128-fold convolution of the 1-day return. No additional fitting
 255 parameters were used to obtain the 128-day return from the 128-fold convolution of the
 256 best fit 1-day Student's t -distribution, Fig. 1. A better fit can be obtained by starting
 257 with a Student's t -distribution with a smaller shape parameter ν than the shape parameter
 258 obtained from the best fit to the 1-day returns. A smaller ν broadens the tails for the 128-fold
 259 convolution. The best fit distribution parameters were used to demonstrate that the n -day
 260 return is to a good approximation the n -fold convolution of the 1-day return. A smaller ν
 261 can be justified on the basis that the 1-day return is the convolution of the tic-by-tic returns.
 262 The tic-by-tic returns will be described by distributions with small shape parameters, i.e.,
 263 have fat tails, which when convolved to obtain the distribution for the daily adjusted closing
 264 value will be described by distributions with larger shape (or smaller degrees of freedom)
 265 parameters. The best fit Student's t -distribution to the 1-day returns provides a convenient
 266 starting point. The shape of a repeatedly self-convolved Student's t -distribution and the
 267 rate that a repeatedly self-convolved Student's t -distribution approaches a normal pdf are
 268 dependant on the truncation and the shape parameter [17].

269 4 Prices of European Call Options

270 Table 3 gives C_o , the price of an n -day European call option, as determined from the solution
 271 $S(t)$ to the homogeneously saturated equation, Eq. (2), for noise driving terms $f(t)$ that
 272 follow a Student's t -distribution (top half of the table) or normal pdf (bottom half of the
 273 table). For comparison C_o as predicted by the Black-Scholes equation is given in the right
 274 hand column. For all the pricing, the best fit parameters obtained for the fits to the S&P
 275 500 data were used. These best fit parameters are given in the bottom portion of Table 2 in
 276 Sec. 3. To calculate prices, the following values were assumed: the price of the asset at time
 277 zero $S_o = \$50.00$; the strike price at time $T = n$ days $K_T = \$49.00$; one year was taken as

278 252 days; and, the risk free rate $r = 0.03$ per year.

279 The expectation $E\{\max(S_T - K_T, 0)\}$ was calculated by numerical integration to obtain
280 $C_T = \exp(r \times T/252) C_o$ for a T -day option. Monte Carlo simulation yielded similar results.
281 The pdf was divided into 1000 sections of equal area between 10^{-3} and 0.999, and was
282 evaluated at areas of 1.0×10^{-5} , 2.5×10^{-5} , 5.0×10^{-5} , 1.0×10^{-4} , 2.5×10^{-4} , and 5.0×10^{-4}
283 and the symmetrical points near unity. Except for values beyond 0.99999, the required
284 values of $S_T(x)$ were found from numerical solution to Eq. (2). For contributions from
285 values beyond 0.99999, a linear approximation $S_T(x) = S_T(0) + qx/\beta$ was multiplied by
286 the analytic expression for the pdf for S_T and integrated to infinity. q was the input scale
287 parameter reported in Table 1. The pdf for S_T was obtained by using the defining equation
288 for the T -day linear return R_T , $R_T = 1000 \times (S_T/S_o - 1)$, and transforming the best-fit
289 pdf for R_T . Trapezoidal integration was employed to determine the expectation. Here the
290 notation $S_T(x)$ indicates that the price of the asset $S(t)$ is to be evaluated for $\alpha t + W(t) = x$
291 and at an expiry time T . The value of the subscript T has no bearing on the solution to the
292 price. The subscript T indicates the shape of the pdf to associate with the price.

293 The values for C_o in Table 3 show a dependence on β , with C_o decreasing with an increase
294 of β and the effect becoming more pronounced as n of n -day increases. These dependencies
295 on β and n owe to noise rectification. The values in the tail of the distribution push the
296 solution into the non-linear region. This gives a non-zero value to the output noise (the
297 input noise has a mean value of zero) and this increases the mean value of the solution. The
298 noise rectification was not controlled in the calculations reported in Table 3. The amount
299 of rectification increases as the width of the input distribution increases. This explains the
300 increase with n . For $T = 128$ days, the mean value for $S(T)$ was calculated as \$51.374
301 for $\beta = 0.001$ and \$51.098 for $\beta = 3.0$ for a noise driving term that follows a Student's
302 t -distribution. For normally distributed noise, the mean values for $S(T)$ were found to be
303 \$51.031 and \$50.770. The true value was $S_o \exp(0.03 T/252) = \$50.7677$.

Table 3: C_o from the solution $S(t)$ to Eq. (2) for noise drawn from a Student's t -distribution and from a normal distribution. For comparison, C_o as determined from the Black-Scholes equation is displayed. $S_o = \$50.00$ and $K_T = \$49.00$.

	$\beta = 0.001$	$\beta = 0.01$	$\beta = 0.1$	$\beta = 0.3$	$\beta = 1.0$	$\beta = 3.0$	Black Scholes
t							
1-day	1.025	1.020	1.018	1.018	1.018	1.018	
22-day	1.527	1.516	1.508	1.505	1.504	1.504	
44-day	1.910	1.895	1.869	1.865	1.863	1.862	
88-day	2.543	2.520	2.476	2.467	2.466	2.463	
128 day	3.242	3.196	3.125	3.109	3.102	3.100	
normal							
1-day	1.008	1.007	1.007	1.006	1.006	1.006	1.0061
22-day	1.488	1.481	1.469	1.467	1.466	1.466	1.4529
44-day	1.874	1.861	1.840	1.836	1.835	1.834	1.8162
88-day	2.531	2.508	2.472	2.459	2.455	2.455	2.4261
128-day	3.207	3.167	3.104	3.090	3.083	3.082	3.0361

304 Values for C_o calculated using the best-fit t -distributions are greater than the prices
305 found from the normal pdf and from the Black-Scholes equation. The values of C_o found for
306 the normal distribution using Eq. (2) are similar to the values found from the Black-Scholes
307 equation. In the Black-Scholes equation, the stock price is assumed to follow a log-normal
308 distribution. For the normal distribution and the homogeneously saturated equation, the
309 stock price follows a normal distribution. Pinn [18] considered pricing of options when the
310 distribution of the prices of the underlying stock followed a Student's t -distribution.

311 Values for C_o were also found for numerical integration of the S&P 500 returns, in contrast
312 to numerical integration of the best-fit distribution. These values are listed in Table 4 along
313 with the Black-Scholes prices. The numerical integration of the S&P 500 data leads to larger
314 values for the price of the option ($S_o = \$50.00$, $K_T = \$49.00$; $r = 0.03$ per year, best-fit
315 volatility) than is obtained from integration of the best fit distributions.

316 Table 5 gives values of C_o for values of the strike K_T for the homogeneously broadened
317 equation with t and normal statistics, for the Black-Scholes equation, for direct numerical
318 integration of the S&P 500 data, and for a Gosset [12] formula. For these calculations,

Table 4: C_o from numerical integration of S&P 500 data and from the Black-Scholes equation. $S_o = \$50.00$ and $K_T = \$49.00$.

	1-day	22-day	44-day	88-day	128-day
S&P data					
C_o	1.163	1.647	2.243	2.642	3.509
Black Scholes					
C_o	1.006	1.453	1.816	2.426	3.036

Table 5: C_o for different strike prices and methods of calculation with $T = 22$ days, $\beta = 0.3$, and $S_o = \$50.00$.

K_T	t	normal	Black-Scholes	S&P data	Gosset
40.0	10.120	10.107	10.105	9.830	10.11
42.5	7.626	7.614	7.611	7.427	7.613
45.0	5.144	5.122	5.119	5.075	5.131
47.5	2.743	2.702	2.693	2.822	2.726
50.0	0.861	0.836	0.834	1.031	0.856
52.5	0.141	0.103	0.111	0.276	0.150
55.0	0.022	0.004	0.005	0.108	0.026
57.5	0.004	0.000	0.000	0.035	0.005
60.0	0.001	0.000	0.000	0.002	0.001

319 $\beta = 0.3$, $S_o = 50.0$, $r = 0.03$, and $n = 22$. The Gosset formulae price European call options
320 when the underlying stock price is distributed as a log-Student's t -distribution. The Gosset
321 formulae truncate the underlying pdf or cap the value of the stock to keep the integrals
322 involved in the pricing finite. For the calculations presented in Table 5 the t -distribution
323 was truncated at $p = 0.9999$. For the 22-day best fit parameters of $\nu = 6.3$ and $b = 34.7$,
324 this yields truncation of per mille returns of > 266 . From Table 2 the maximum 22-day per
325 mille return was 224, which includes an average return of 7. Thus the truncation for the
326 Gosset formula is reasonable.

327 The five methods predict similar trends and results, with the exception of the direct
328 numerical integration of the S&P 500 data. The numerical integration of the S&P data gives
329 a decreasing price for $K_T \leq \$45.0$. $K_T = \$45.0$ maps to a per mille return of -100 . From
330 Fig. 7, it can be observed that the calculation of the expectation required for the price starts

331 to access the left hand shoulder on the 22-day return. This will bias the calculation towards
332 smaller values of $S_T - K_T$ and reduce C_o .

333 5 Conclusion

334 A homogeneously saturated equation that gives the time development of the price of an asset
335 was presented and used to price European call options. The options were priced using best-fit
336 Student's t -distributions and best-fit normal distributions to linear returns calculated from
337 the daily adjusted closing values for the S&P 500 Index from 3 January 1950 to 27 July 2011.
338 The prices as predicted by the homogeneously saturated equation were compared to prices
339 obtained from direct integration of the S&P 500 data, from the Black-Scholes equation, and
340 from a Gosset formula, and were found to be in agreement.

341 The homogeneously saturated equation borrows from laser physics. The homogeneously
342 saturated equation is similar to the equation for the output of a simple, homogeneously
343 broadened laser. The homogeneously saturated equation for the time development of the
344 price of an asset was justified by solution in steady state of coupled rate equations that
345 describe a reservoir of money that can be used to purchase an asset and the stock price. A
346 noise driving term was added to the rate equation for the reservoir of money. The equations
347 thus describe the effect of a fluctuating money supply on the price of the asset.

348 The homogeneously saturated equation for the time development of the price of an asset
349 has some interesting and realistic features. In the limit that a saturation parameter β , which
350 is a measure of the strength of the coupling of the reservoir and price of the asset, equals
351 zero, the standard equation for the time development of the price of an asset is obtained.
352 The solution to the standard equation is geometric motion, or geometric Brownian motion,
353 if the noise forcing term $\sigma f(t)$ follows normal statistics.

354 The solution to the homogeneously saturated equation tends, through the saturation

355 inherent to the form of the coupled equations, to depend linearly on the input to the model
 356 for input x such that $S(x) \gg 0$ and to compress the output. Fluctuations in the input to the
 357 homogeneously saturated equation create smaller fluctuations in the solution for non-zero β .
 358 The transfer function of the homogeneously saturated equation goes as x/β where x is the
 359 input to the equation for x such that $S(x) \gg 0$. This is in contrast to the standard model,
 360 where the output $S(t) = \exp(\int \sigma f(t) dt)$ depends exponentially on the input. With the
 361 standard model and with a noise forcing term (i.e., the input) that follows fat tailed statistics
 362 (such as the Student's t -distribution, which is known to fit well the returns), integrals that
 363 are required to price European call options are infinite . The homogeneously saturated
 364 equation, through linearization and compression by saturation of the reservoir, does not
 365 suffer the same shortcoming as the standard model. In this respect the homogeneously
 366 saturated equation for the development in time of the price of an asset corresponds to reality
 367 better than the standard model, and thus should be preferred over the standard model for
 368 the development in time of the price of an asset.

369 **6 Appendix**

370 In this Appendix, rate equations for a reservoir of money $M(t)$ that is available to invest in an
 371 asset with price $S(t)$ and for the time development of the price of the asset are constructed.
 372 The rate equations are written as Langevin equations, which are first order differential equa-
 373 tions with noise driving terms. The Langevin equations should be interpreted as integral
 374 equations [19, pg 172] [20, Ch 10.2]. Average values found by the Langevin approach are
 375 identical to solutions found by Ito's calculus [20].

376 Let $M(t)$ be the amount of money that is available to invest in an asset. Let N be
 377 the rate at which money is pumped into the reservoir of money $M(t)$ that can be used to
 378 purchase the asset and let $\beta/\tau \times M(t) \times S(t)$ be the rate that money is removed from the

379 reservoir owing to purchases of the asset. Let τ be a characteristic time constant that allows
 380 for money to be removed or added to the reservoir, depending on whether $M(t)$ is greater
 381 than or less than some value M_o . Allow for a noise driving term $\sigma/\tau f(t)$.

382 A rate equation for $M(t)$ is then

$$\frac{d}{dt}M(t) = N - \frac{\beta}{\tau} \times S(t) \times M(t) - \frac{M(t) - M_o}{\tau} + \frac{\sigma}{\tau} f(t). \quad (6)$$

383 All parameters in the rate equation have a time dependence, but it is assumed that these
 384 parameters change slowly in time. Thus each point in time is assumed to evolve about a
 385 steady state . In steady state, the time derivative equals zero and

$$M(t) = \frac{N + \frac{M_o}{\tau} + \frac{\sigma}{\tau} f(t)}{\frac{1}{\tau} + \frac{\beta}{\tau} S(t)} = \frac{(\alpha + \sigma f(t))}{1 + \beta S(t)}. \quad (7)$$

386 In the last form for $M(t)$ the symbol α has been defined. The equation for the time
 387 development of the value of an asset becomes

$$\frac{d}{dt}S(t) = M(t) S(t) = \frac{\alpha S(t) + \sigma S(t) f(t)}{1 + \beta S(t)}. \quad (8)$$

388 In this approach the noise is ascribed to fluctuations in the amount of money available
 389 to invest in the asset. The value at time t of an asset under this homogeneously saturated
 390 approach is $S(t)$, the solution to Eq. (2).

391 Note that the interaction between the reservoir and the rate that money left the reservoir
 392 was defined as β/τ where τ is a characteristic time constant of the reservoir. This definition
 393 defines β in terms of a characteristic time τ of the system and suggests that a reasonable
 394 value for β might be of order unity.

7 References

References

- [1] D. T. Cassidy, “Analytic description of a homogeneously broadened injection laser”, IEEE J. Quantum Electron. QE-20, (1984) 913–918.
- [2] D. T. Cassidy, “Homogeneously saturated model for development in time of the price of an asset”, submitted July 2011.
- [3] J.-P. Bouchaud, J. D. Farmer, and F. Lillo, “How Markets Slowly Digest Changes in Supply and Demand.” *Handbook of Financial Markets: Dynamics and Evolution*, 57–156, T. Hens and K. Schenk-Hoppe, editors, Elsevier: Academic Press, 2009.
- [4] E. Smith, J. D. Farmer, L. Gillemot, and S. Krishnamurthy, “Statistical theory of the continuous double auction”, *Quantitative Finance* 3 (2003) 481–514.
- [5] B. Toth, Z. Eisler, F. Lillo, J.-P. Bouchaud, J. Kockelkoren, and J. D. Farmer, “How does the market react to your order flow?”, 4 April 2011, arXiv:1104.0587v1
- [6] M. G. Daniels, J. D. Farmer, L. Gillemot, G. Iori, and E. Smith, “Quantitative Model of Price Diffusion and Market Friction Based on Trading as a Mechanistic Random Process”, *Phys. Rev. Lett.* 90 (2003) 108102.
- [7] C. Anteneodo and R. Riera, “Additive-multiplicative stochastic models of financial mean-reverting processes”, *Phys Rev E* 72 (2005) 026106.
- [8] F. Wu, X. Mao, and K. Chen, “A highly sensitive mean-reverting process in finance and the Euler-Maruyama approximations”, *J. Math. Anal. Appl.* 348 (2008) 540–554.
- [9] S. M. Ross, *Introduction to Probability Models*, 9th edition, Academic Press, 2007, Chapter 10.

- 417 [10] B. de Finetti, “Foresight: Its Logical Laws, Its Subjective Sources”, in *Studies in Sub-*
418 *jective Probability*, H. E. Kyburg, Jr. and H. E. Smokler, editors, John Wiley & Sons,
419 New York, p. 103, 1963.
- 420 [11] D. Heath and W. Sudderth, “On a theorem of de Finetti, oddsmaking, and game the-
421 ory”, *Ann. Math. Stat.* 43 (1972) 2072–2077.
- 422 [12] D. T. Cassidy, M. J. Hamp, and R. Ouyed, “Pricing European options with a log
423 Student’s t -distribution: a Gosset formula”, *Physica A* 389 (2010) 5736–5748.
- 424 [13] J.-P. Bouchaud and D. Sornette, “The Black-Scholes option pricing problem in mathe-
425 matical finance: generalization and extensions for a large class of stochastic processes”,
426 *J. Phys. I France* 4 (1994) 863–881.
- 427 [14] J. L. McCauley, G. H. Gunaratne, and K. E. Bassler, “Martingale option pricing”,
428 *Physica A* 380 (2007) 351–356.
- 429 [15] D. T. Cassidy, “Effective truncation of a Student’s t -distribution by truncation of the
430 chi distribution in a chi-normal mixture”, *Open Journal of Statistics*, 2 (2012) 519–525.
- 431 [16] D. T. Cassidy, M. J. Hamp, and R. Ouyed, “Student’s t -distribution based option
432 sensitivities: Greeks for the Gosset formulae”, arXiv:1003.1344 (2009).
- 433 [17] D. T. Cassidy, “Describing n -day returns with Student’s t -distributions”, *Physica A*
434 390 (2011) 2794–2802.
- 435 [18] K. Pinn, “Minimal variance hedging of options with Student- t underlying”, *Physica A*
436 276 (2000) 581-595.
- 437 [19] W. T. Coffey, Yu. P. Kalmykov, and J. T. Waldron, *The Langevin Equation: with*
438 *Applications to Stochastic Problems in Physics, Chemistry, and Electrical Engineering*,
439 Second Edition, World Scientific Publishing Co. Pte. Ltd., (2004).

440 [20] M. Lax, W. Cai, and M. Xu, *Random Processes in Physics and Finance*, Oxford Uni-
441 versity Press, New York, (2006).